Ultraviolet photorefractivity features in doped lithium niobate crystals

Haijun Qiao, Jingjun Xu,* Guoquan Zhang, Xinzheng Zhang, Qian Sun, and Guangyin Zhang
Photonics Center, College of Physics Science, Nankai University, Tianjin 300071, People's Republic of China and TEDA Applied Physics School, Nankai University, Tianjin 300457, People's Republic of China
(Received 15 December 2003; revised manuscript received 22 April 2004; published 2 September 2004)

In this work we studied photorefractive effect of lithium niobate ($LiNbO_3$) doped with Zn, In, and Na at ultraviolet (UV) wavelength down to 351 nm. It is found that the UV photorefraction of $LiNbO_3$ doped with Zn, In, or Na was enhanced significantly as compared to that of the nominally pure $LiNbO_3$. Our results show that the statement that the property of resistance against photorefraction in highly Zn and In doped $LiNbO_3$ is correct only in visible light range. By contrary, these crystals exhibit as excellent photorefractive characteristics in UV. We also find that there are doping concentration threshold values of Zn and In for the disappearance of the light-induced lens-like effect both in visible and in UV, but such concentration threshold values are not found for UV photorefraction within the highest doping concentrations we used. In highly Zn or In doped $LiNbO_3$ crystals, diffusion dominates over photovoltaic effect and electrons are determined to be the dominant charge carriers in UV photorefraction. The results are of interest to the study on the defect structure of $LiNbO_3$. Further investigation on this field is greatly urgent.

DOI: 10.1103/PhysRevB.70.094101 PACS number(s): 77.84.Dy, 42.70.Nq, 42.70.Ln

I. INTRODUCTION

Lithium niobate ($LiNbO_3$) crystals remain as the promising versatile materials in optic, electro-optic and photonics science and technology. They are widely used in optical doubler and optical parametric oscillators, holographic data storage, and even for acoustical memory as recently reported.[1] Since researchers in Bell Laboratories observed "an optically-induced inhomogeneity in the refractive index of $LiNbO_3$ and other ferroelectrics"[2] in 1966, a lot of investigations have been done on this material. The topics ranged from macro- to micro-mechanism, and from basic defect structures to various applications.

The optically-induced damage and photorefractive effect are two notable and important characters of $LiNbO_3$. Both of them mean that in this material the photo-induced change in the refractive index is reversible even under low light intensity. In application, lithium niobate crystals with enhanced photorefraction or with optical-damage-resistance need different requirements, respectively. For example, lithium niobate crystals with high optical-damage-resistance are adopted for frequency doubling, especially for the promising PPLN (periodically poled lithium niobate) used in quantum information[3] and second-harmonic generation processing;[4] on the other hand, crystals with high photorefractive sensitivity and low light-induced noise scattering are needed for holographic data storage. As is well known, photorefraction of $LiNbO_3$ could be modified by doping the crystals with appropriate impurities. It is believed that, as far as the effect on photorefraction of $LiNbO_3$ is considered, dopants could be divided into two groups: Dopants such as Fe, Co, Mn and Cu tend to enhance the photorefraction, whereas those such as Mg, Zn, and In tend to reduce the photorefraction, i.e., the crystal shows optical-damage-resistance and photorefractive resistance. Investigations have been done in this field for several years, and presently it is commonly believed that the strength of the photorefractive effect of $LiNbO_3$ is determined by the corresponding intrinsic or external defects of the crystals. Although well-known conclusions have been made and several theories are brought forward to support them,[5–7] many aspects still remain unclear so far, especially the defect centers responding for the ultraviolet (UV) photorefraction in $LiNbO_3$. The incomplete knowledge prevents one from efficiently utilizing the material.

The UV photorefraction of nominally pure $LiNbO_3$ was reported in 1992.[8] Later Laeri *et al.* made an review on UV photorefraction in various ferroelectrics in 1995.[9] They reported that the photorefraction of pure $LiNbO_3$ due to the diffusion mechanism is enhanced in UV as compared to that in visible, and the dominant charge carriers in UV are holes. In 2000 Xu *et al.* reported an enhancement of UV photorefraction in highly magnesium doped $LiNbO_3$[10] which, however, shows a perfect optical-damage-resistance in the visible region. These phenomena were not fully understood up to now. Since the UV photons can excite electrons or holes from deeper levels rather than photons of visible region, in this sense the UV photorefraction of $LiNbO_3$ provides another window to look into the crystalline defect structure. Moreover, this study would be helpful for manufacturing good-property materials in application of the UV photorefractivity. In this paper, we carried out a comprehensive study on the UV photorefraction of doped $LiNbO_3$. Such a study would be helpful to identify and to understand the UV photorefractively sensitive defect centers in $LiNbO_3$.

II. EXPERIMENTS DETAILS

Congruent pure $LiNbO_3$ crystals doped with several different concentrations of In and Na were grown by Czochralski technique from the congruent melt. After being poled the crystals were cut into Y-sheets whose thickness is 3.5 mm and both XY-surfaces were polished. The Zn-doped $LiNbO_3$ crystals were provided by Russian Academy of Science and similar aftergrowth treatments were introduced to the

TABLE I. List of the lithium niobate crystals and their dopants used in our experiment.

Abbreviation	Dopant	Concentration (mol%)	Dimensions ($x \times y \times c, mm$)
CLN	None	0	$10 \times 3 \times 10$
CZn5[a]		5.4	$4 \times 2 \times 5$
CZn7[a]	Zn	7.2	$4 \times 2 \times 5$
CZn9[a]		9.0	$7 \times 2 \times 4$
CIn1		1.0	$7 \times 3.5 \times 7$
CIn3	In	3.0	$5 \times 3.5 \times 5$
CIn5		5.0	$7 \times 3.5 \times 7$
CNa1		1.0	$7 \times 3.5 \times 6$
CNa3	Na	3.0	$7 \times 3.5 \times 6$

[a]The three crystals were grown in Institute of Crystallography of the Russian Academy of Sciences.

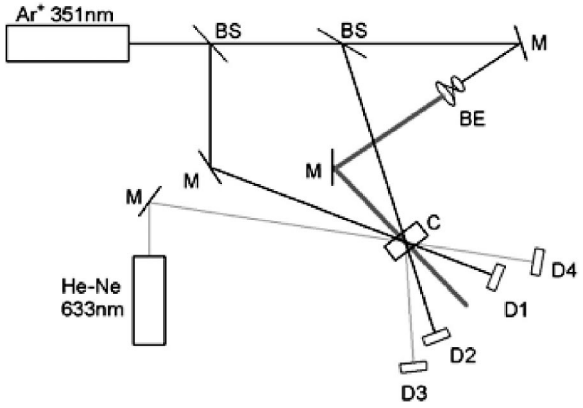

FIG. 1. The experiment configuration for the UV photorefraction measurement. M: mirror, BS: beam splitter, BE: beam expander, C: crystal, D1–D4: detectors.

samples. A Y-sheet of congruent pure undoped $LiNbO_3$ crystal was prepared for comparison. In Table I we listed the samples used in our experiments and abbreviation of each sample in the following statement is given as well. All the doping concentrations listed in Table I were the concentrations in the melt. The $+c$-axis direction was determined according to the pyroelectric effect. Because the energy transferring direction was often taken as an indication of the type of the dominant charge carriers type,[11] the determination of the $+c$ direction is of obvious importance. Firstly, we put two sheets of c-cut $LiNbO_3$ crystals, of which one is congruent pure and the other is 6.5 mol % Mg doped $LiNbO_3$, into the etching acid for 12 hours. It is well-known that the $-c$ end is easier etched than $+c$ end, so the $-c$ end becomes more frosted after etching.[12] Thus we can determine the $-c$ direction of these two "standard" pieces of crystal inerrably. Secondly, we heated the two crystals and then cooled them down by putting them into charged printing ink. After photographic fixing, we found that the determined $-c$ end was not contaminated by ink, while the other end ($+c$ end) was covered by an ink film due to the pyroelectric effect and charge neutralization effect. According to the above results, we checked all samples, and the end covered with ink was determined to be $+c$ end of the crystal.

Among our samples, In:$LiNbO_3$ was predicted to be optical-damage-resistant crystals[13] and was confirmed in 1995,[14] and the concentration threshold was suggested to be about 5 mol % in the melt by the authors of Ref. 15. The concentration thresholds for Zn and Mg were reported at about 7 to 8 mol %[16] and about 5 mol % for Mg.[17,18] These three kinds of optical-damage-resistant impurities are believed to affect the photorefractive properties of $LiNbO_3$ almost in the same way: They tend to enhance the photoconductivity greatly, to induce a blue-shift the absorption edge, and to enhance the resistance against optical-damage. As for the Na-doped $LiNbO_3$, few publications[19,20] can be found. It is probable that the $LiNbO_3$:Na crystals are difficult to grow due to the big difference in the radii of Li^+ (0.65 Å) and Na^+ (0.91 Å). Kong *et al.*[19] reported that Na:$LiNbO_3$ crystal also illustrates a decrease in photorefraction at 488 nm comparing with the congruent one. However, it was also reported that an increase in Na doping concentration was not accompanied by a decrease instead of an increase in optical-damage-resistance. Concerning the particularity of Na, we also performed some experiments with these Na-doped samples. Although Na seems not an effective optical-damage-resistance impurity in $LiNbO_3$, it may be interesting for investigating defect structures in $LiNbO_3$. The infrared absorption (characterizing the OH^- vibration) spectra of the samples listed in Table I were measured. Among our samples, it is found that the OH^- absorption peak in infrared region moves from 3487 to 3508 cm^{-1} in sample CIn5, and moves from 3483 to 3530 cm^{-1} in both CZn7 and CZn9. This indicated that the doping concentrations of samples CIn5, CZn7, and CZn9 are above the threshold, while those in other samples are under the threshold.

We used two-wave coupling scheme to study the UV photorefraction of our samples. The whole experiment configuration is shown in Fig. 1. Ar^+ laser operating at 351 nm was selected as the working beam. We split the output laser beam into three beams, and then intersected two of them with extraordinary polarizations inside the samples and wrote a photorefractive grating. We always kept the photorefractive grating vector K parallel to the c-axis. The third beam was expanded and served as the uniform erasing beam incident at off-Bragg angle when necessary. The formation and decay of the gratings were monitored by a weak He-Ne laser beam (wavelength at 632.8 nm) incident at the Bragg angle. During the measurement, we let the two writing beams and the weak probe beam incident on the crystal at the same time. To avoid a disturbance of the probe beam, we kept its intensity as weak as possible, only about $1.0-1.4\ mW/cm^2$. By this means, we could observe the formation and decay of the gratings by recording the diffracted beam intensity of the probe beam, e.g., by the detector D3 shown in Fig. 1. The diffraction efficiency η of the light-induced grating was measured by simply blocking one of the writing beams after saturation. Here η is defined as $\eta=(I_d+I_i)/I_i$, where I_d is the diffracted beam intensity, and I_i is the transmitted beam intensity. We measured the intensities of transmitted and diffracted beams just after blocking one writing beam, in order

TABLE II. The measured photorefractive characteristics of our samples.

Samples	CLN	CZn5	CZn7	CZn9	CIn1	CIn3	CIn5	CNa1	CNa3
Photoconductivity σ_{ph} ($\times 10^{-12}$ cm/$\Omega\cdot$W)	3.32	10.6	25.2	57.3	1.59	7.46	12.9	2.01	0.96
Diffraction efficiency[a] η (%)	9.05	16.9	22.3	25.3	10.1	15.9	17.7	7.5	18.1
Photorefractive response time[b] τ_e (s)	12.4	1.97	1.01	0.88	13.9	3.06	1.68	11.3	22.2
Two-wave coupling gain[c] Γ(cm^{-1})	1.32	11.0	15.2	21.7	1.16	11.8	17.0	1.54	1.95
Photorefractive sensitivity[a] S (cm/J)	0.99	4.0	8.85	11.1	0.86	2.85	3.88	0.56	0.38
Dynamic range[a] $M/\#$	0.14	0.11	0.12	0.14	0.26	0.19	0.15	0.11	0.17

[a]The intersect angle in the air $2\theta=40°$, corresponding to photorefractive grating period $\Lambda=0.5$ μm, two recording intensity $I_S=121.7$ mW/cm^2 and $I_R=176.9$ mW/cm^2, respectively.
[b]The response time constants were measured under the uniform UV illumination of 70.8 mW/cm^2.
[c]The intensity ratio between the reference and signal beam I_R:I_S was 100:1.

to prevent the self-enhancement or self-depletion[21,22] from bringing up inaccuracy to the results. Considering the energy transferring between the two writing beams, we did not record the gratings with equal intensity writing beams, but used a configuration with unequal intensities according to Ref. 23. According to Kogelnik's coupled wave theory,[24] we could calculate the amplitude of refractive index change Δn from $\eta=\sin^2[\pi\Delta n d/(\lambda\cos\theta)]$, where θ is the half intersection angle of the two writing beams. In the two-wave coupling experiment, we turned off the probe and erasing beams and only let the two writing beams illuminate the crystals at the same time, and modulated the intensity ratio of the two beams around 100:1. The two-wave coupling gain was obtained through relation $\Gamma=(1/d)\ln[(I_S'I_R)/(I_SI_R')]$, where the subscripts S and R denote signal and reference beams (here the signal beam is the one with a low intensity in the following description), I_S', I_R' and I_S, I_R are the transmitted intensities of the two writing beams with and without coupling, respectively, d is the thickness of the grating, e.g., the thickness of the sample in our case. The photoconductivity $\sigma_p(I)$ was estimated by fitting the intensity dependence of erasure time constant τ_e for grating in terms of the relation $\sigma_p=\varepsilon\varepsilon_0/\tau_e$, where ε_0 is the vacuum dielectric constant and ε is the relative dielectric constant. Here the erasure time constant τ_e is defined as the time when the diffraction efficiency decays to $1/e$ of its initial value. We also estimated the dark conductivity σ_d by the relation $\sigma_d=\varepsilon\varepsilon_0/\tau_d$, where τ_d is the decay time constant of the grating in darkness. The photorefractive sensitivity S is an important parameter for the photorefractive material and describes how much energy is needed to produce a given refractive index change. S is defined as $S=(1/Id)(d\sqrt{\eta}/dt)|_{t=0}$, where I is the total recording intensity. The dynamic range $M/\#$ is a parameter describing the storage capacity of the photorefractive gratings, in other words, it stands for how many gratings can be recorded inside a unit volume. $M/\#$ here is defined as $M/\#=\tau_e(d\sqrt{\eta}/dt)|_{t=0}$. The term $d\sqrt{\eta}/dt|_{t=0}$ in the two equations above means the gradient of square root of diffraction efficiency at the very beginning of the recording.

III. PHOTOREFRACTION OF DOPED $LiNbO_3$ IN ULTRAVIOLET

From the overall experimental results in UV, the samples exhibited UV photorefractive properties which are different from those in visible. The UV photorefractive characteristics of our samples are listed in Table II. The photorefractive effect in these highly Zn and In doped crystals was enhanced significantly in UV as compared to that of the pure ones, whereas different influences were also observed for different dopants in $LiNbO_3$. In this section, we emphasize the description of the comparison of the photorefractive properties in UV with those in visible and the comparison of photorefractive properties in doped crystals with those in pure one.

A. Zn doped congruent $LiNbO_3$

Zinc is +2 valence dopant in $LiNbO_3$. The photorefractive effect of Zn:$LiNbO_3$ in visible is pretty weak, especially when the doping concentration is over the threshold as in CZn7 and CZn9. However, the Zn:$LiNbO_3$ crystals show very strong UV photorefractive effect and are excellent materials for UV photorefraction.

From Table II, we note a drastic increase of the photoconductivity in Zn:$LiNbO_3$, for example, it is as high as 57.3 $\times 10^{-12}$ cm/$\Omega\cdot$W in the sample CZn9. In the sample CZn9, the response time is as short as 0.88 s at the total recording intensity of 70.8 mW/cm^2. With increase of Zn concentration, other photorefractive properties such as diffraction efficiency, coupling gain, and recording sensitivity are also greatly enhanced. The recording and optical erasing cycle is shown in Fig. 2(b). A long time evolution of the recording process is also given in Fig. 3(b), in which no remarkable disturbance is found. From Fig. 2(b) we can see that the gratings can be recorded and erased in Zn:$LiNbO_3$ in a very short interval. The photorefractive sensitivities of Zn:$LiNbO_3$ samples were measured and listed in Table II. Comparing with that in CLN, the sensitivity is much improved by the Zn doping. The sample CZn9 exceeds all other samples and shows the largest UV photorefractivity, see Table II. The dark decay processes of gratings are shown in Fig. 4(b). It is obvious that, besides the photoconductivity and diffraction efficiency, the dark conductivity also increases with the increase of Zn concentration in the crystal.

Figure 5(a) shows the evolution of the transmitted signal beams in Zn:$LiNbO_3$ samples during light amplification experiments with an external crossing angle $2\theta=40^\circ$. A coupling gain coefficient Γ up to 21.7 cm^{-1} was observed in CZn9. To our knowledge, this is the largest gain coefficient

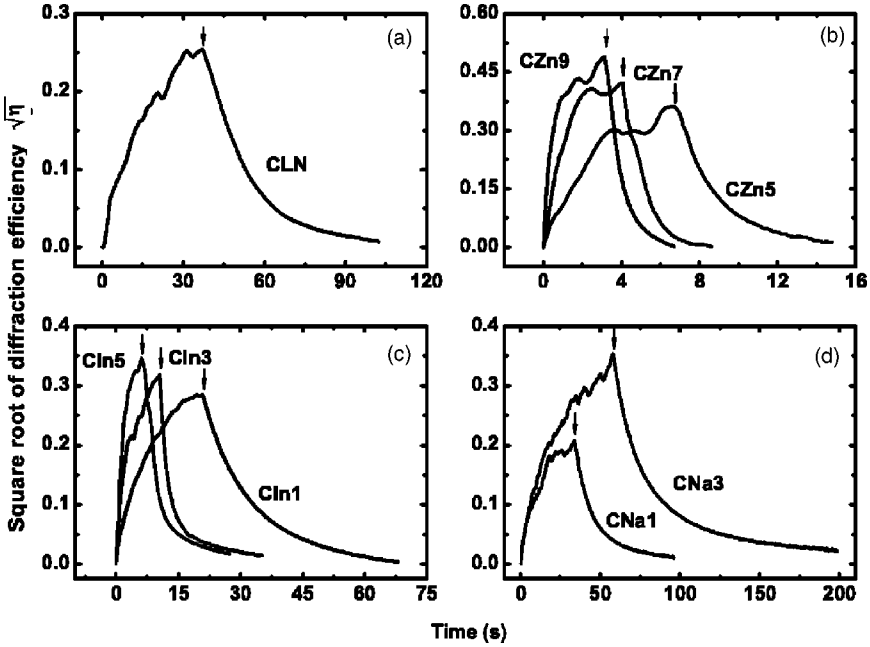

FIG. 2. Holographic recording and optical erasure cycle with the same intensity in our samples. The intensities of two recording beams are 121.7 and 176.9 mW/cm^2 for (a) CLN, (b) $Zn:LiNbO_3$, and (c) $In:LiNbO_3$, 120.2 and 152.5 mW/cm^2 for (d) $Na:LiNbO_3$, respectively, and the external crossing angle $2\theta=40°$. The small arrows indicate the time of decay beginning.

in UV reported in $LiNbO_3$ crystals. Note that we could only observe slight light amplification in CLN under the same configuration. We found the light energy transfer unidirectionally toward $-c$-axis in all $Zn:LiNbO_3$ samples in our experiment. This result was reproducible in all the $Zn:LiNbO_3$ samples. This indicates that diffusion is the dominant mechanism and electrons are the dominant charge carriers during the UV photorefractive processes in $Zn:LiNbO_3$. We noted that this conclusion is inconsistent with the results reported earlier,[25,26] where the holes were supposed to be the dominant charge carriers in $Zn:LiNbO_3$ with Zn concentration higher than 7.5 mol % under the illumination of a 488 nm laser beam. The dependence of the two-wave coupling gain coefficient Γ on the grating period Λ ($\Lambda=\lambda/2\sin\theta$) was also measured and shown in Fig. 5(b). As known, the relation between the two-wave coupling gain coefficient and the beam-crossing angle is described by $\Gamma=A\sin\theta\cos 2\theta_{in}/(1+B^{-2}\sin^2\theta)\cos\theta_{in}$,[27] where $2\theta_{in}$ and 2θ are the internal and external beam-crossing angle, respectively, $A=\gamma_{eff}\xi(8\pi^2n^3k_BT/e\lambda^2)$, $B=(e\lambda/4\pi)(N_{eff}/\varepsilon\varepsilon_0k_BT)^{1/2}$, ξ is electron-hole competition factor, N_{eff} is the effective charge density. By fitting the measured Λ-dependence of Γ using the function given above, we obtain the effective trap center concentrations N_{eff}. The fitting curves are also shown in Fig. 5(b). One should notice that high-order diffracted beams appeared due to phase-mismatching with grating spacing Λ greater than 1.2 μm. So those data were not taken in the fitting. The effective trap density N_{eff} is fitted to be $0.51\times10^{16}\,cm^{-3}$ for the sample CZn5, $1.07\times10^{16}\,cm^{-3}$ for CZn7, and $2.81\times10^{16}\,cm^{-3}$ for CZn9. It is clear that intro-

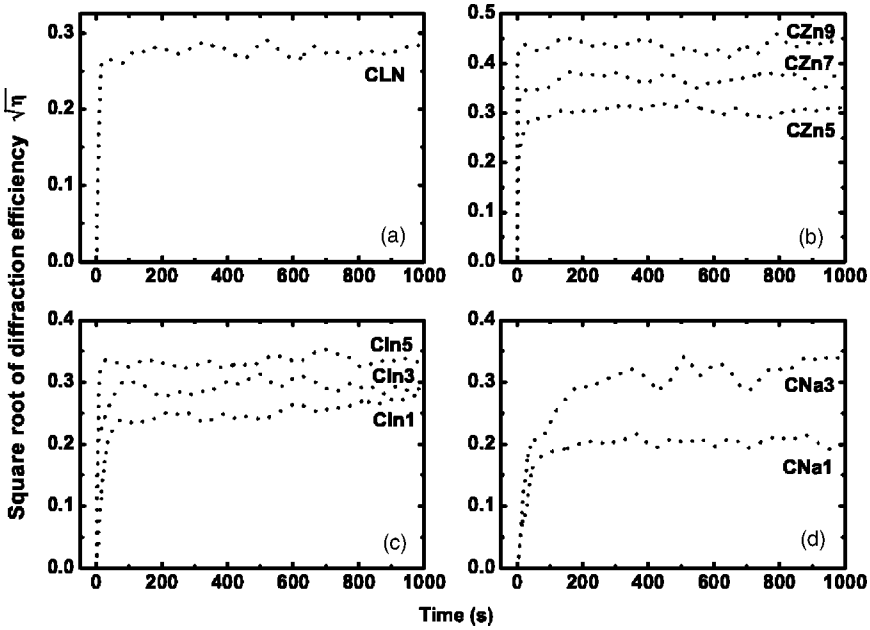

FIG. 3. Long time recording of holograms recorded in our samples, the external crossing angle $2\theta=40°$.

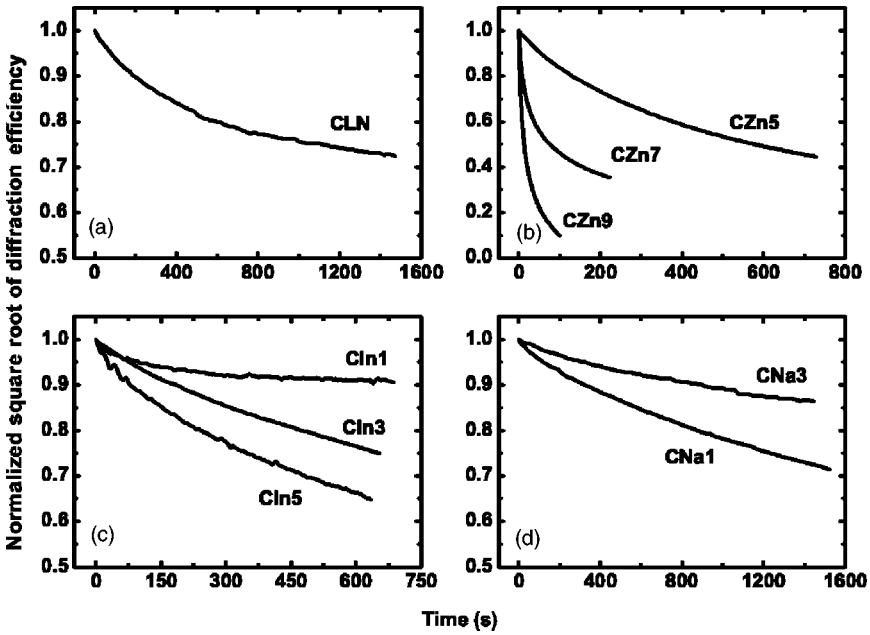

FIG. 4. Dark decay of holograms recorded in our samples, only the weak He-Ne probing beam is open.

ducing Zn into $LiNbO_3$ brings a noticeable increase in the density of effective trap centers for photorefraction in UV.

We could also see from Table II that the sensitivity is greatly improved by Zn doping. The sensitivity as high as 11.1 cm/J was achieved in the sample CZn9. The dynamic range of Zn:$LiNbO_3$, however, is not large because of the short erasing time due to a very high photoconductivity. Highly Zn doped $LiNbO_3$ crystals are suitable for the dynamic and real-time holographic application in UV.

In brief, the UV photorefractive effect of Zn:$LiNbO_3$ is strong and totally different from its visible behaviors. Zn:$LiNbO_3$ crystals show high photorefractive sensitivities and are good photorefractive materials in UV. They also indicate that there are some unknown defect structures in $LiNbO_3$ crystals responsible for UV photorefraction.

B. In doped congruent $LiNbO_3$

Indium is +3 valence dopant and is considered as the most efficient dopant to suppress the photorefraction of $LiNbO_3$ in visible due to the lowest threshold concentration. From the experimental results, In:$LiNbO_3$ crystals also show an enhanced UV photorefraction, although not so high as that in Zn:$LiNbO_3$.

In general, the same measurements as for Zn:$LiNbO_3$ were done to the In:$LiNbO_3$ samples. The results are also shown in Table II. It is seen that the photoconductivity, the diffraction efficiency, the two-wave coupling gain coefficient, and the photorefractive sensitivity also increase with the increase of In concentration. As mentioned above, the In doping concentration of sample CIn5 is above the threshold, and those of CIn1 and CIn3 are below the threshold. We

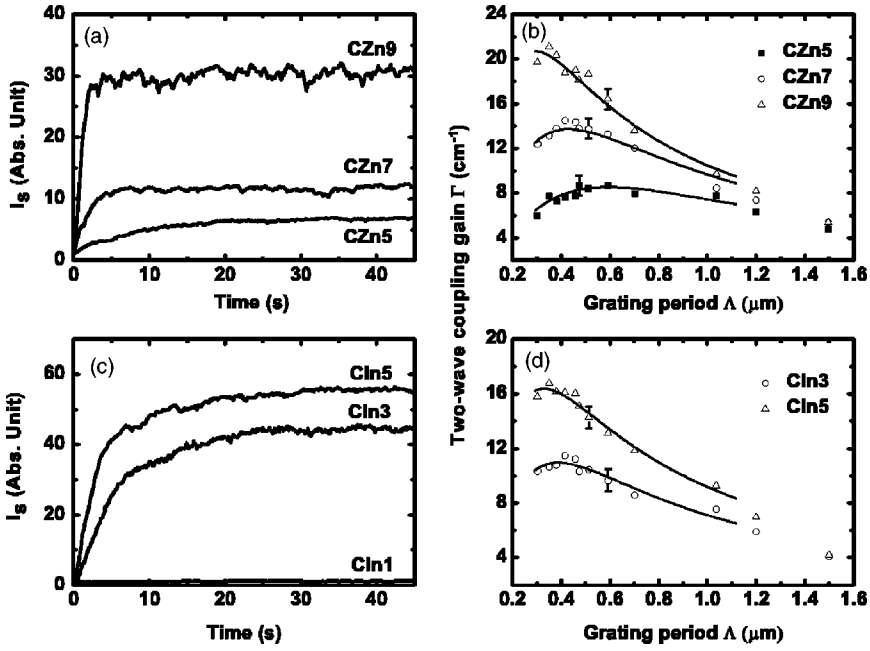

FIG. 5. The light amplification in our samples: (a),(c) Time dependence of the amplified signal beams I_S in Zn:$LiNbO_3$ and In:$LiNbO_3$ at incident angle $2\theta = 40°$, the intensity ratio between the reference beam and signal beam is 100:1; (b),(d) dependence of two-wave coupling gain Γ on grating period Λ in Zn:$LiNbO_3$ and In:$LiNbO_3$, and the solid curves are the theoretical fitting results.

notice that the photoconductivity and photorefractive sensitivity of CIn5 are lower than those of CZn7 and CZn9, only close to CZn5 whose Zn doping concentration is below the threshold. Figure 2(c) shows the recording and erasing cycle of the recorded grating and the long time recording process is given in Fig. 3(c). As to the little perturbance of η during the long time recording in all the samples, we considered that it was perhaps caused by the disturbance of the environment, or some competing mechanisms may exist. We also show in Fig. 4(c) the dark decay process of the recorded grating. Comparing Fig. 4(c) with Fig. 4(b), it is seen that photorefractive gratings in $In:LiNbO_3$ can be preserved much longer than those in $Zn:LiNbO_3$, indicating that the dark conductivity in $In:LiNbO_3$ is much lower than that in $Zn:LiNbO_3$. We notice that the dark decay time constant of grating in CLN is even shorter than that in CZn1 but is approximate to that in CZn3.

The In concentrations in sample CIn1 and sample CZn3 are below the threshold. We could not observe light amplification in CIn1, whereas a $\Gamma = 11.0\ cm^{-1}$ was found in CZn3, as shown in Fig. 5(c) which shows the time evolution of the transmitted signal beam in the light amplification experiment. Note that a large gain coefficient is also observed in the sample CIn5. It seems that the concept of concentration threshold for optical-damage-resistance in visible is no longer valid in UV. During the two-wave coupling experiments, energy always transferred towards $-c$ direction in samples CIn3 and CIn5, which indicates that electrons are dominant charge carriers in these crystals. The Λ-dependence of Γ of CIn3 and CIn5 are shown in Fig. 5(d) and they are fitted by using the same function as that used in the case for $Zn:LiNbO_3$. The effective trap densities are fitted to be $1.37\times10^{16}\ cm^{-3}$ for CIn3 and $2.10\times10^{16}\ cm^{-3}$ for CIn5, respectively. Note that high-order diffraction appeared again at large grating spacing and these data were not considered in the theoretical fitting.

We should remind here that the fitting function is a result based on the pure diffusion mechanism. In the samples CLN and CIn1 we observed fairly high diffraction efficiency but negligible beam coupling. Consequently the UV photorefraction in these two crystals is probably based on photovoltaic effect.

The UV photorefraction in highly In-doped $LiNbO_3$ is also enhanced although it is not as effective as those in highly Zn-doped $LiNbO_3$. At the same time, with the increasing of the In doping concentration, diffusion turns to dominant mechanism over other mechanisms. We also notice that the concept of concentration threshold for In in visible is no longer valid for photorefraction in UV.

C. Na doped congruent $LiNbO_3$

Sodium is +1 valence dopant. $Na:LiNbO_3$ crystals showed different behaviors from the two formers in UV photorefractive experiment. Two samples of CNa1 and CNa3 were used in our experiment. They were studied in visible by Kong *et al.* in 1997[19] and it was reported that $Na:LiNbO_3$ showed optical-damage-resistance or photorefractive resistance compared to the congruent pure $LiNbO_3$. However, the ability to resist the opically-induced damage became weaker with increasing Na concentration. So Kong *et al.* supposed that Na is not a good optical-damage-resistant impurity.

Based on two-wave coupling configuration, we measured the UV photorefractive properties of CNa1 and CNa3. The diffraction efficiency was achieved with the two writing beam intensities of 121.7 and 152.5 mW/cm^2, respectively. Figure 2(d) shows the typical grating recording and erasing cycle. The temporal evolution of a long time scale is also shown in Fig. 3(d). The saturated diffraction efficiency for the sample CNa3 is nearly twice as that of CNa1. For the long time recording, the diffraction efficiency did not vary much after it reached the saturation. In general, the photoconductivity in $Na:LiNbO_3$ is lower than that in $Zn:LiNbO_3$ or $In:LiNbO_3$. From Table II, it is seen that the sample CNa3 exhibits a higher diffraction efficiency but lower photoconductivity than CNa1. This phenomenon is different from that in $Zn:LiNbO_3$ and $In:LiNbO_3$, in which the increasing of diffraction efficiency accompanies with the increasing photoconductivity. The dark conductivity in Na-doped $LiNbO_3$ is also very low, as can be inferred from the dark decay curves in Fig. 4(d). The dark decay time constant of gratings in CNa1 is approximately the same as that in CLN, while it is much larger in CNa3. In the light amplification experiment, we set the intensity ratio of two writing beams to be 1:1 and 100:1, respectively. In both cases the two-wave coupling gain coefficient Γ is negligibly small. So we suggested that the main charge transport mechanism is the photovoltaic effect but not diffusion in both CNa1 and CNa3. This conclusion is also valid for CLN as well. The calculated sensitivity and dynamic range are also listed in Table II. It seems that doping $LiNbO_3$ with Na does not improve the recording sensitivity. Although the sample CNa3 has a fairly high diffraction efficiency and a long dark decay time constant which might be favorable for holographic storage, the low sensitivity may be a barrier for such applications.

$Na:LiNbO_3$ crystals exhibit different UV photorefractive properties from $Zn:LiNbO_3$ or $In:LiNbO_3$. With the increase of Na doping concentration, the saturated diffraction efficiency increases while the photoconductivity decreases. On the other hand, contribution from diffusion is negligible and any light amplification cannot be observed during the two-wave coupling. Such difference probably results from the +1 valence of sodium which is identical to that of lithium.

IV. LIGHT-INDUCED SCATTERING AND LENS-LIKE EFFECT OF DOPED $LiNbO_3$ IN UV

Light-induced scattering (LIS) occurring in volume photorefractive crystals is believed to be a charateristic of photorefractive materials. LIS is explained as the amplified weak scattered light due to the gratings recorded by the incident light and its scattered lights in non-local response medium,[28,29] or due to a multi-wave mixing among the incident light and its scattered lights in local response medium.[30] One often evaluates a photorefractive crystal according to its LIS characteristics. However, for applications such as optical storage and light amplification, LIS is a noise source that induces serious deterioration. On the other hand, lens-like

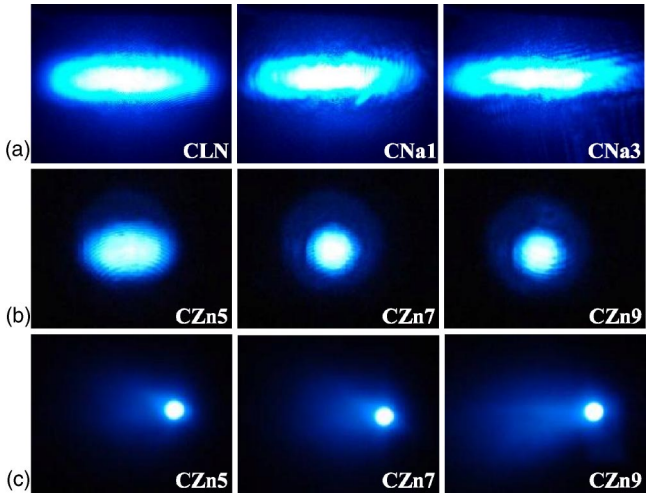

FIG. 6. (Color online) Pictures of LLE and LIS in CLN, Na:$LiNbO_3$ and Zn:$LiNbO_3$: (a) Beam deformation after passing through CLN, CNa1, and CNa3 with focusing beams; (b) beam deformation after passing through CZn5, CZn7, and CZn9 with focusing beams; (c) LIS in CZn5, CZn7, and CZn9 with extra-polarized laser beam.

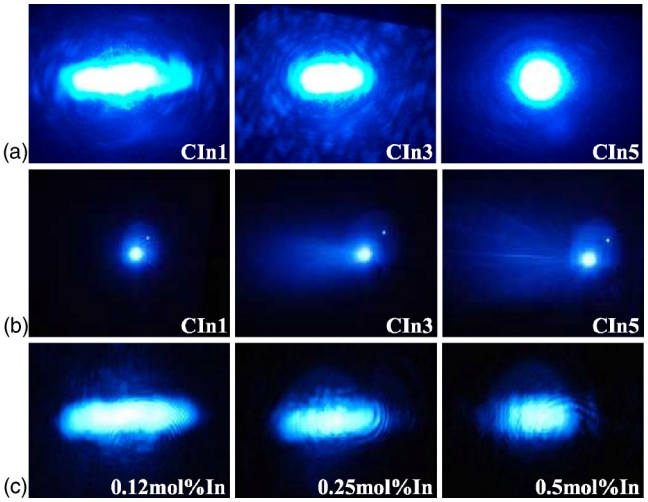

FIG. 7. (Color online) Pictures of lens-like and light induced scattering in In:$LiNbO_3$: (a) Beam deformation after passing through CIn1, CIn3, and CIn5 with focusing beam; (b) LIS in CIn1, CIn3, and CIn5 with extra-polarized laser beam; (c) beam deformation after passing through In:$LiNbO_3$ crystals grown in Russia with focusing beam.

effect (LLE) in photorefractive crystals is slightly different from LIS. Here LLE includes self-focusing or self-defocusing effects in the crystal. LLE is often used to check the ability of resistance against light-induced damage of a material simply by a focused Gaussian laser beam[31,32] and by means of this method Kong *et al.* proved that the threshold intensity for the appearance of optical damage in In:$LiNbO_3$ of an In concentration of 5 mol % was two orders higher than that of the congruent pure $LiNbO_3$.[15] Although both LIS and LLE are due to the diffraction of the incident beam from parasitic gratings recorded in the crystal, they have different characteristics. However, one often thinks that LIS and LLE are two accompanying phenomena, or even confuse them as the same one. Indeed, both LIS and LLE are suppressed in visible in $LiNbO_3$ crystals such as Mg:$LiNbO_3$, Zn:$LiNbO_3$ and In:$LiNbO_3$ when the impurity concentration is over the threshold value. But this is not the case for $LiNbO_3$ in UV.

First, we introduced a focused extraordinarily polarized laser beam and put the samples near to the rear focal plane of the lens to observe the LLE. We could completely eliminate LIS by moving the crystal near to rear focal plane of the lens because of the "speckle size effect" for LIS.[33] The profiles of the light spots deteriorated after passing through all our samples, as shown in Figs. 6(a), 6(b), and 7(a), where the intensity density of incident UV light was 23.9 kW/cm^2. It is found from Figs. 6(a) and 6(b) that LLE is strong in CLN and Na:$LiNbO_3$, while it is suppressed in CZn5 and completely disappears in CZn7 and CZn9 with an available intensity of 23.9 kW/cm^2. The results shown in Fig. 7(a) are similar to what Kong *et al.* obtained at 488 nm.[15] The laser beam passed through the crystal CIn5 without any distortion while it was seriously deteriorated after passing the other two In-doped crystals. We also did the same measurement on three additional In-doped $LiNbO_3$ crystals which were also provided by Russia Academy of Science. These three new samples contain less In concentrations which are denoted in Fig. 7(c). It is shown in Fig. 7(c) that the serious beam distortion occurs in these crystals. The less is the In concentration inside, the larger is the distortion. We measured the intensity threshold of the LLE for our samples and the results are listed in Table III. From the table we see the samples CIn5, CZn7, and CZn9 have very high intensity thresholds which are beyond total output intensity of the laser. Here we may come to a conclusion that in UV LLE of $LiNbO_3$ can be suppressed by Zn or In doping. This conclusion is in consistent with that in visible, e.g., LLE of Zn or In doped $LiNbO_3$ is suppressed both in visible and in UV. CNa1 and CNa3 are somewhat different from others. The sample CNa3 shows a lower threshold than CNa1. Na is not an effective dopant to resist the optical damage as compared with Zn or In. This is also valid in visible.[19] As for as the LLE effect is considered the threshold characters in UV and in visible are the same.

Secondly, we moved the focusing lens away and let the extraordinarily polarized and collimated laser beam illuminate the crystals directly. In this case LIS occurred, as shown in Figs. 6(c) and 7(b). Among our samples, we could not

TABLE III. The intensity threshold of the LLE at 351 nm in our samples.

Samples	CLN	CZn5	CZn7	CZn9	CIn1	CIn3	CIn5	CNa1	CNa3
Threshold[a] (kW/cm^2)	0.09	17.9	>23.9	>23.9	0.16	10.9	>23.9	0.13	0.078

[a]The highest value is limited by the maximum output of our laser— 23.9 kW/cm^2.

observe LIS in CLN, CNa1, CNa2, and CIn1. This is in consistence with the results obtained in the light amplification experiment because the two-wave coupling gain coefficients are negligibly small. No LIS could be observed in the three additional In:$LiNbO_3$ samples either. In the rest four samples, e.g., CZn7, CZn9, CIn3, and CIn5, strong asymmetric scattering fanning toward $-c$-axis direction was observed and it became stronger with the increase of Zn or In concentrations in the crystal. Such results agree well with the results of light amplification in Sec. III and Table II. We may also draw a conclusion that the dominant charge carriers in these samples are electrons. It is seen that the results of LIS in UV are exactly contrary to those in visible.

V. DISCUSSION

It seems to be a well-known result that holes are the dominant charge carriers in congruent pure $LiNbO_3$ in UV photorefractive effect[8,9] and in highly Zn doped $LiNbO_3$ in visible.[26] However, we notice the energy transferring direction is always toward the $-c$-axis direction during the two-wave coupling experiments for the samples Zn:$LiNbO_3$ and In:$LiNbO_3$ in which fairly large coupling gain coefficient Γ was observed. This indicates that in these samples diffusion is the dominant charge transport mechanism and the light-excited electrons are the dominant charge carriers. This is inconsistent with what was reported by Jungen and Laeri.[8,9]

Here we summarize briefly the similarities and the differences between LLE and LIS in visible and those in UV. In visible, both LLE and LIS are suppressed in Zn:$LiNbO_3$ and In:$LiNbO_3$ with the doping concentration over their respective threshold. In CZn7, CZn9, and CIn5, both LLE and LIS are negligible in visible. However, in UV LIS in them becomes stronger, although LLE is still suppressed as in the case in visible. In other words, LIS in Zn or In doped $LiNbO_3$ crystals has the contrary concentration dependence in visible and in UV, while LLE has similar concentration dependence. The threshold value of the doping concentration is valid for LLE both in visible and in UV but no longer valid for LIS in UV. But in Na:$LiNbO_3$ crystals, the results are different. The laser beam distortion due to LLE does not become better in CNa1 and CNa3 compared with that in CLN, neither in visible nor in UV. LIS cannot be observed in them either. In a word, Na:$LiNbO_3$ crystals exhibit the similar properties of LLE and LIS in visible and in UV, which is not as the case of Zn or In doped crystals.

As is known, LLE and LIS are different behaviors resulting from the same origin—photorefractivity. Here we do not consider thermal lensing for the following reason. Thermal lensing originates from the thermal-optic effect. In general, the response time of the thermal lensing is very short in the order of 10^{-9} s. The response time of both LLE and LIS are in the order of subsecond in our experiments. So we could exclude the contribution from thermal lensing. Therefore, both LLE and LIS result from the diffraction of the incident beam on parasitic gratings recorded due to the photorefractive effect of the crystals. The difference is that LIS occurs from gratings with different spatial frequencies (usually high) recorded by the incident beam and coherent noise beams, while in our case LLE is restricted only to gratings with low frequencies recorded by different components of the incident focusing beam. Therefore, LLE is observed only at small angle from the direction of the transmitted beam, and LIS is observed at a wide range of diffractive angles. In our opinion, the essential difference between them is that LLE is connected with the photovoltaic effect and LIS results from diffusion. LLE disappears in CZn7, CZn9, and CIn5 because the photovoltaic effect decreases significantly in them due to the increase of photoconductivity and dark conductivity. At the same time, with a larger photoconductivity the crystal shows a higher sensitivity and a shorter response time, which is desired for the real-time applications. By doping Zn or In the photoconductivity of $LiNbO_3$ crystal is greatly enhanced especially when the doping concentration is over the threshold value. Whereas, the dopant Na is not a good candidate to make a $LiNbO_3$ crystal with high photoconductivity. What should be reminded of is that we did not consider the variation of the Glass constant which might be changed by doping $LiNbO_3$ with different dopants of different concentrations.

On the other hand, with the decrease in the photovoltaic field of Zn:$LiNbO_3$ and In:$LiNbO_3$, the diffusion field dominates over the photovoltaic field especially at large recording angles. As is well known, diffusion leads to unidirectional energy transferring via two-wave coupling. Therefore, in our experiment unidirectional LIS in large angle range could be observed in Zn:$LiNbO_3$ and In:$LiNbO_3$ samples except for CIn1 (seen in Figs. 6 and 7). However, in CLN, CNa1, CNa3, and CIn1, the photoconductivity is not high enough. Comparing to the photovoltaic effect, the contribution from diffusion is still neglectable so unidirectional LIS was not observed in these four samples. But, the reason why diffusion field should be enhanced with the increase of Zn or In doping concentration still remains unclear to us.

According to the above results on LLE and LIS, Zn or In doped $LiNbO_3$ crystals are able to find new applications in UV. For instance, in highly Zn-doped $LiNbO_3$ crystals, one can take advantage of the greatly enhanced photorefractive sensitivity in UV but does not need to care about LLE of the crystal any longer.

In general, when two coherent laser beams intersected in the samples, amplitude gratings due to the light-induced absorption (LIA) and phase gratings due to the photorefractivity may be recorded. A characteristic of the photorefractive effect, which distinguishes it from other mechanisms, is the nonzero phase shift between the refractive-index grating and the light interference pattern for holographic recording without an external electric field. This phase shift would result in a unidirectional energy transfer between the interacting beams, while absorption gratings can only cause simultaneous changes in the intensities. We did the LIA experiment according to the configuration of Ref. 34 and no obvious LIA could be observed in all our samples. Furthermore, we estimated the amplitude of the refractive index change Δn according to the relations $\eta=\sin^2[\pi\Delta n d/(\lambda\cos\theta)]$ and $\Gamma=2(\pi\Delta n/\lambda)\sin\phi$, respectively (we estimate ϕ to be $\pi/2$), in those samples two-wave coupling gain coefficient Γ could be measured. We found that Δn were approximately the same in both cases. All the above results show that the amplitude of

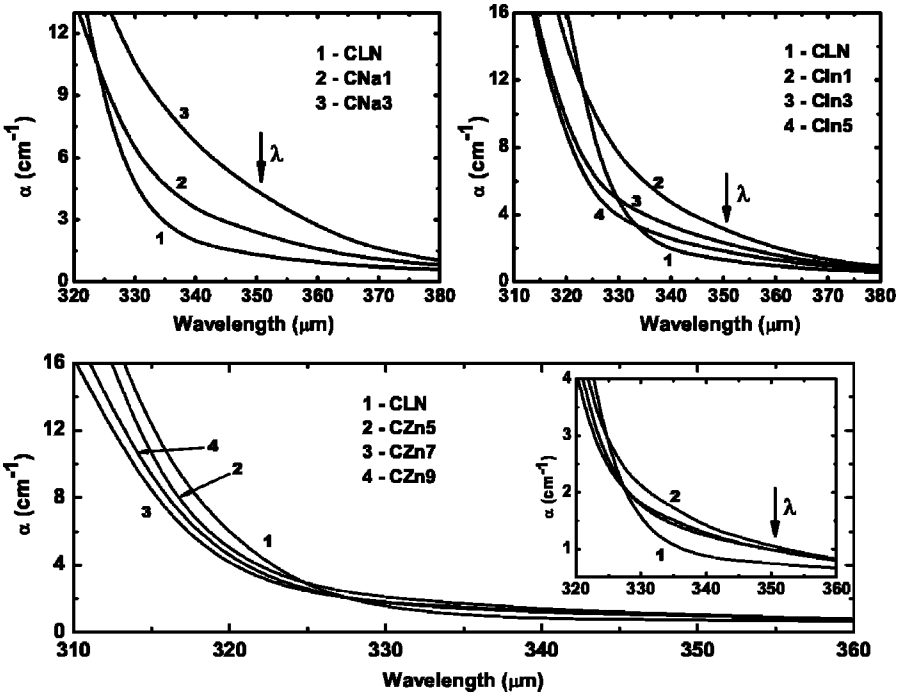

FIG. 8. The absorption spectra near the absorption edge of our samples, the wavelength indicated by the small arrows is our recording wavelength—351 nm.

the absorption grating is negligibly small as compared to that of the photorefractive gratings in our case. Therefore, in the following discussions we consider only the photorefraction.

According to the results described above, we can see that in the samples CLN, CIn1, CNa1 and CNa3, the photovoltaic effect is the dominant contribution to the photorefractivity, while in CZn7, CZn9, and CIn5, diffusion played the key role, and in CZn5 and CIn3, there is a competition between the two mechanisms. Due to the strong influence from the high-order diffraction at large grating spacings (small recording angles), we cannot get direct evidences of competition between these two mechanisms. In our opinion, no matter it is a congruent pure crystal or the doped ones, the increasing photoconductivity results directly in the decrease of the photovoltaic field and therefore the increase of contribution from diffusion. According to the results of Ref. 9, with the same light intensity, photoconductivity of $LiNbO_3$ in UV is larger than that in visible. In the samples CLN, CIn1, CNa1, and CNa3, the diffraction efficiency η is independent of the recording angle or the grating spacing. This is a typical property resulting from the photovoltaic space-charge field. When the dopants like Mg, Zn, or In are introduced, photoconductivity in crystals is enhanced and photovoltaic field decreases, and diffusion becomes gradually the dominant mechanism.

In comparison with that in visible, the samples show a significant enhancement in UV photorefractivity. We think that it is probably because the high energy of UV photons can excite charge carriers from some new UV photorefractive centers. Then what are the new photorefractive centers?

According to the Li-vacancy model,[35] in congruent pure $LiNbO_3$ an intrinsic defect of Nb_{Li} (Nb-antisite) is compensated by four V_{Li} (Li-vacancy). As is believed that when impurities like Mg, Zn, or In incorporate into $LiNbO_3$, they firstly repel the Nb_{Li} to the normal site and at the same time form the new extrinsic defects of Mg_{Li}, Zn_{Li}, or In_{Li}. As a matter of fact, the concentration threshold for optical-damage-resistance in visible corresponds to the vanishing of Nb_{Li}.[36] In other words, when the doping concentration is higher than the threshold, there is no Nb_{Li} any more in the crystal. Considering that the UV photorefraction is enhanced dramatically in samples CZn7, CZn9, and CIn5 whose doping concentrations are already higher than the threshold, the new UV photorefractive centers should not be related to Nb_{Li} centers. With regard to the extrinsic defects Mg_{Li}, Zn_{Li}, or In_{Li}, we do not think that they may act as the UV photorefractive centers because they are monovalence so that electrons or holes are not able to be excited from or trapped on them. In a word, the UV photorefractive centers should be related to some defect structures other than intrinsic defects of Nb_{Li} and extrinsic defects of Mg_{Li}, Zn_{Li}, or In_{Li}.

In 2000, Lee *et al.* reported a UV-sensitive deep center in near stoichiometric $LiNbO_3$ codoped with Tb and iron.[37] This UV-sensitive center could be considered as an electron donor/acceptor under the UV illumination. However, they did not give other information on the microstructure of this UV-sensitive center.

Recently Vikhnin *et al.* demonstrated an exciton structure theoretically and experimentally in ABO_3-type ferroelectric oxides, and they named it as CTVE (charge transfer vibronic excitons).[38] They believe that CTVE is composed of a pair of an electron polaron and a hole polaron and it can be treated as a deep-level center with its energy level located just above the top of the valence band. We measured the absorption spectra for all the samples, and the spectra are shown in Fig. 8. Considering the possible different growing conditions in two crystal-grown groups, we chose two congruent pure $LiNbO_3$, one was grown by us and the other was grown in Russian Academy of Science, respectively, for a more reasonable comparison of the absorption spectra. One sheet of congruent pure $LiNbO_3$ with a thickness of 3 mm grown by us was compared with the $In:LiNbO_3$ and $Na:LiNbO_3$, and

another sheet with a thickness of 1.2 mm grown in Russian Academy of Science was compared with the $Zn:LiNbO_3$. That is the reason of different values of absorption coefficient for congruent pure $LiNbO_3$ in Fig. 8. The absorption edge moves to shorter wavelengths with Zn-In doping, yet the absorption coefficients at 351 nm are still larger than the congruent pure one and the fact indicates an existence of some deep-level centers. Anyway, only from Fig. 8 we cannot verify the existence of CTVE structure in our samples. Other mechanisms such as multi-centers models may also be possible. Although many results are still unclear, the UV photorefractive properties in $LiNbO_3$ give insight into to the deep-level centers in the crystal. Further detailed investigations on the defect structure of $LiNbO_3$ are necessary to clarify the UV photorefractivity.

Before the conclusion, we offer some comments on the $Na:LiNbO_3$ crystals. $Na:LiNbO_3$ crystals exhibited different UV photorefractive properties from $Zn:LiNbO_3$ and $In:LiNbO_3$. Such differences perhaps come from the different influence of Na and Zn-In on defect structures of $LiNbO_3$. Na is a monovalence element, which does not need a charge compensation when it enters Li-site. It may firstly occupy Li-site and repel the Nb_{Li} to the normal Nb-site. The defects of Nb_{Li} and V_{Li} decrease sharply, and the absorption edge has a blue-shift in CNa1. With the increase in Na doping concentration, no more Nb_{Li} or V_{Li} are removed, and the basic spatial arrangement of $LiNbO_3$ does not permit more Na ions. Anyway, the situation in Na-doped $LiNbO_3$ crystals is much more complicated than that in Zn and In doped $LiNbO_3$ crystals. We do not have ideas on the explanation of the abnormal behaviors of UV photorefraction of Na-doped $LiNbO_3$ crystals so far.

VI. CONCLUSION

In conclusion, in this work we studied the UV photorefractive features in three types of doped lithium niobate crystals and found that the properties of photorefractive effect in UV are far different from that in visible. UV photorefraction is enhanced in the so-called optical-damage-resistant crystals, such as Zn and In doped $LiNbO_3$, and their optical-damage-resistance and the threshold for resistance are only effective in visible. From another aspect, these crystals especially $Zn:LiNbO_3$ with fast response are excellent candidates for UV photorefractive applications. Based on the character of optical-damage-resistance in visible and a photorefraction enhancement in UV, $LiNbO_3$ crystals doped with appropriate impurities are probably an outstanding platform for the microstructure fabricated in UV and can be used in visible. This work also leads us a new scope for defect structures in Zn and In doped $LiNbO_3$ crystals, although the defects related to light-induced charge carriers process in UV are not clear yet. Investigation on this field is greatly needed for understanding the famous and versatile optical material—$LiNbO_3$.

ACKNOWLEDGMENTS

This work is sponsored by the "973" project (G1999033004) of China, Tianjin Key Technique Project (Grant Nos. 0031002311 and 003108911), The National Natural Science Foundation of China (Grant Nos. 6010801 and 60308005), the Key Project of the National Natural Science Foundation of China (Grant No. 10334010), the Excellent Young Teachers Program of MOE, P.R.C. (Grant No. 2002-350), and the Special Foundation of Education Committee for Excellent Teachers. Thanks to Professor Romano Rupp from Vienna University for his very helpful advice and discussion. Thanks to Professor Tatyana Volk from Russian Academy of Science for her $LiNbO_3$ crystals. Thanks to Professor Jean Pierre Huignard and Professor Brigitte Loiseaux in Thales Research and Technology (France) for helpful discussion.

*Electronic address: jjxu@nankai.edu.cn

[1] M. S. McPherson, I. Ostrovskii, and M. A. Breazeale, Phys. Rev. Lett. **89**, 115506 (2002).
[2] A. Ashkin, G. D. Boyd, J. M. Dziedzic, R. G. Smith, A. A. Ballman, J. J. Levinstein, and K. Nassau, Appl. Phys. Lett. **9**, 72 (1966).
[3] S. Tanzilli, W. Tittel, H .D. Riedmatten, H. Zbinden, P. Baldi, M. D. Micheli, D. B. Ostrowsky, and N. Gisin, Eur. Phys. J. D **18**, 155 (2002).
[4] K. R. Parameswaran, J. R. Kurz, R. V. Roussev, and M. M. Fejer, Opt. Lett. **27**, 43 (2002).
[5] E. Krätzig, Ferroelectrics **21**, 635 (1978).
[6] O. F. Schirmer, O. Thiemann, and M. Wöhlecke, J. Phys. Chem. Solids **52**, 185 (1991).
[7] T. R. Volk and M. Wöhlecke, Ferroelectr. Rev. **1**, 195 (1998).
[8] R. Jungen, G. Angelow, F. Laeri, and C. Grabmaier, Appl. Phys. A: Solids Surf. **55**, 101 (1992).
[9] F. Laeri, R. Jungen, G. Angelow, U. Vietze, T. Engel, M. Würtz and D. Hilgenberg, Appl. Phys. B: Lasers Opt. **61**, 351 (1995).
[10] Jingjun Xu, Guangyin Zhang, Feifei Li, Xinzheng Zhang, Qian Sun, Simin Liu, Feng Song, Yongfa Kong, Xiaojun Chen, Haijun Qiao, Jianghong Yao, and Zhao Lijuan, Opt. Lett. **25**, 129 (2000).
[11] P. Günter and J. P. Huignard, *Photorefractive Materials and Their Applications I* (Springer-Verlag, Berlin, 1989).
[12] A. Prokhorov and Y. S. Kuzminov, *Physics and Chemistry of Crystalline of Lithium Niobate* (Adam Hilger, 1990).
[13] T. R. Volk and N. Rubinina, Ferroelectr., Lett. Sect. **109**, 345 (1992).
[14] T. R. Volk, M. Wöhlecke, N. Rubinina, N. V. Razumovskii, F. Jermann, C. Fischer, and R. Böwer, Appl. Phys. A: Mater. Sci. Process. **60**, 217 (1995).
[15] Y. Kong, J. Wen, and H. Wang, Appl. Phys. Lett. **66**, 280 (1995).
[16] T. R. Volk, V. I. Pryalkin, and N. M. Rubinina, Opt. Lett. **15**, 996 (1990).
[17] G. G. Zhong, J. Jian, and Z. K. Wu, Proceedings of the Eleventh International Quantum Electronics Conference, IEEE, New York, 631 (1980).

[18] D. A. Bryan, R. Gerson, and H. E. Tomaschke, Appl. Phys. Lett. **44**, 847 (1984).
[19] Y. F. Kong, J. K. Wen, and Z. F. Yang, Chin. Phys. Lett. **14**, 629 (1997).
[20] Haijun Qiao, Jingjun Xu, Yongfa Kong, Qian Sun, and Guangyin Zhang, OSA Trends in Optics and Photonics **62**, 139 (2000).
[21] T. K. Gaylored, T. A. Rabson, F. K. Tittel, and C. R. Quick, J. Appl. Phys. **44**, 896 (1973).
[22] M. Segev, A. Kewitsch, A. Yariv, and G. A. Rakuljic, Appl. Phys. Lett. **62**, 907 (1993).
[23] Y. Liu, L. Liu, and C. Zhou, Opt. Lett. **25**, 551 (2000).
[24] H. Kongelnic, Bell Syst. Tech. J. **48**, 2909 (1969).
[25] H. Wang, J. Wen, J. Li, and H. Wang, Appl. Phys. Lett. **57**, 344 (1990).
[26] J. Deng, J. Wen, Z. Wu, and H. Wang, Appl. Phys. Lett. **64**, 2822 (1994).
[27] M. D. Ewbank, R. R. Neurgaondar, W. k. Cory, and J. Feinberg, J. Appl. Phys. **62**, 374 (1987).
[28] É. M. Avakyan, K. G. Belabaev, and S. G. Odulov, Sov. Phys. Solid State **25**, 1887 (1983).
[29] R. A. Rupp and F. W. Drees, Appl. Phys. B: Photophys. Laser Chem. **39**, 223 (1986).
[30] G. Zhang, G. Tian, S. Liu, J. Xu, G. Zhang, and Q. Sun, J. Opt. Soc. Am. B **14**, 2823 (1997).
[31] F. S. Chen, J. Appl. Phys. **40**, 3389 (1969).
[32] F. Jermann, M. Simon, and E. Krätzig, J. Opt. Soc. Am. B **12**, 2066 (1995).
[33] G. Y. Zhang, Q. X. Li, P. Pho, S. M. Liu, Z. K. Wu, and R. R. Alfano, Appl. Opt. **25**, 2955 (1986).
[34] S. Wevering, J. Imbrock, and E. Krätzig, J. Opt. Soc. Am. B **18**, 472 (2001).
[35] N. Iyi, K. Kitamura, F. Izumi, J. K. Yamanoto, T. Hayashi, H. Asano, and S. Kimura, J. Solid State Chem. **10**, 340 (1992).
[36] G. Zhang, Y. Kong, and J. Xu, OSA Trends in Optics and Photonics **62**, 194 (2001).
[37] M. Lee, S. Takedawa, Y. Furukawa, K. Kitamura, and H. Hatano, Phys. Rev. Lett. **84**, 875 (2000).
[38] V. Vikhnin, R. Eglits, S. Kapphan, G. Borstel, and E. Kotomin, Phys. Rev. B **65**, 104304 (2002).